ОБЪЕДИНЕННЫЙ
ИНСТИТУТ
ЯДЕРНЫХ
ИССЛЕДОВАНИЙ

ДУБНА

E1 - 11331

INVARIANT CROSS SECTIONS FOR THE INCLUSIVE REACTIONS $\bar{p}p \to \pi^+ + X$ AND $\bar{p}p \to p + X$ AT 22.4 GeV/c

Alma-Ata - Dubna - Helsinki - Moscow - Prague
Collaboration

1978

E1 - 11331

INVARIANT CROSS SECTIONS FOR THE INCLUSIVE REACTIONS $\bar{p}p \to \pi^+ + X$ AND $\bar{p}p \to p + X$ AT 22.4 GeV/c

Alma-Ata - Dubna - Helsinki - Moscow - Prague
Collaboration

Боос Э.Г. и др. E1 - 11331

Инвариантные сечения частиц в инклюзивных реакциях
$\bar{p}p \to \pi^+ + X$ и $\bar{p}p \to p + X$ при 22,4 ГэВ/с

В работе приведены инвариантные сечения для π^+-мезонов и протонов в $\bar{p}p$ -взаимодействиях при 22,4 ГэВ/с. Средняя множественность π^+ -мезонов и протонов равны 1,92±0,02 и 0,41±0,02, соответственно. Спектры частиц в аннигиляционных каналах аппроксимировались с помощью разности в $\bar{p}p$ - и pp-данных. Получившиеся распределения имеют те же общие черты что и полные данные $\bar{p}p$ -взаимодействий.

Работа выполнена в Лаборатории высоких энергий ОИЯИ.

Препринт Объединенного института ядерных исследований. Дубна 1978

Boos E.G. et al. E1 - 11331

Invariant Cross Sections for the Inclusive Reactions
$\bar{p}p \to \pi^+ + X$ and $\bar{p}p \to p + X$ at 22.4 GeV/c

The invariant inclusive cross sections for π^+ mesons and protons from $\bar{p}p$ reactions at 22.4 GeV/c are presented. The average multiplicity for π^+ meson and proton production is 1.92±0.02 and 0.41±0.02, respectively. The annihilation spectra have been approximated using the difference between $\bar{p}p$ and pp data. The resulting distributions have similar gross features as the total $\bar{p}p$ data.

The investigation has been performed at the Laboratory of High Energies, JINR.

Preprint of the Joint Institute for Nuclear Research. Dubna 1978

I. Introduction

Lately great interest has been devoted to inclusive studies of high and medium energy interactions. However, many of these investigations have been limited to a restricted phase space region. In this paper we present the invariant single particle distributions in the whole kinematical region for the reactions

$$\bar{p}p \to \pi^+ + X, \quad (1)$$

$$\bar{p}p \to p + X \quad (2)$$

from bubble chamber "Ludmila" experiment at 22.4 *GeV/c*.

In our previous paper we have given the topological cross sections and multiplicity data [1]. The inclusive spectra for positive and negative particles and slow protons have been also published [2].

In section II we give a short resume of experimental details and discuss the method used for the separation of the proton and π^+ inclusive spectra. In section III we present the invariant inclusive cross sections for π^+s in the variables (x, p_T^2) and (y^*, p_T^2) both in single and double differential form. The proton spectra are given as functions of x, y^* and p_T^2. In section IV we compare our data with the pp data at 24 *GeV/c* and try to describe the main features of the annihilation events.

II. Experimental Procedure

The data presented in this paper have been obtained in an exposure of the 2m HBC "Ludmila" to a RF separated 22.4 *GeV/c* antiproton beam at the Serpukhov accelerator. After two independent scans their discrepancies were resolved in a third scan. The scanning losses were less than 2% for all charged prong topologies. The events were measured on semiautomatic devices and processed through the geometrical reconstruction programs (mass dependent THRESH or HYDRA geometry). The separation between positive pions and protons was made using only the ionization information of a track. Thus we could distinguish between pions and protons up to a laboratory momentum of about 1.2 *GeV/c*. The contamination of other particles is neglected. Altogether 11095 events were used in this analysis. For each topology a weight was calculated to account for the losses during the event processing.

To remove elastic events, we calculated for all two-prong reactions the missing energy ϵ_m as a function of the scattering angle of charged particles. This distribution exhibits a narrow peak centered at $\epsilon_m = 0$ corresponding to the elastic events sitting on a low almost flat background of inelastic events. To reduce this background, we used a compound test on the missing energy, $|\epsilon_m| \leq$ 80 *MeV/c*, and on the opening angle α_{lab} $-0.02 \leq \cos\alpha_{lab} \leq 0.35$, between the secondary particles. Thus we got a sample of 1836 elastic events (the uncetrainty being $\pm$ 80) out of 4326 two-prong events. The $d\sigma/dt$ distribution for our elastic sample was fitted by an exponential, giving the slope $-11.22 \pm 0.34\,(GeV/c)^{-2}$ which is close to the value $-11.7\,(GeV/c)^{-2}$ extrapolated from the data in ref. /3/. After normalization to a total inelastic cross section of 39.1 *mb* /3,4/ our microbarn equivalent is equal to 0.296 weighted events/*mb*.

From simple kinematical considerations we know that pions in the region A of *fig. 1* can be identified. Assuming CP conservation, we get the cms forward-going positive pion spectrum by reflection of the backward-going negative particles (π^-'s account for about 99%)

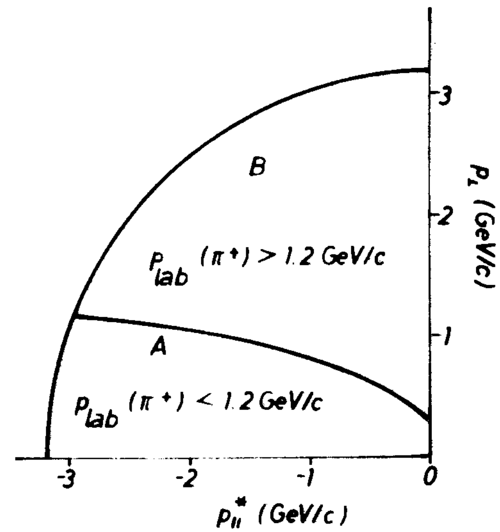

Fig. 1. The Peyrou plot is used for separating π^+ *mesons. All negative particles from the backward part are reflected around* $p_L^* = 0$ *to form the forward part of the inclusive* π^+ *spectrum. In region A the particles can be identified by ionization. In region B the weight* $w(p_L^*)$, *given by eq. (4) in the text, is assigned to the particles to give* π^+ *mesons.*

to the forward hemisphere. In region B positive pions cannot be distinguished from protons. Therefore we introduce the following weighting function:

$$w(p_L^*, p_T) = \frac{N^\pi(p_L^*, p_T)}{N^+(p_L^*, p_T)}, \qquad (3)$$

where N^π is the number of positive pions and N^+ the number of all positive particles transformed to the cms as pions. Outside the region B this function can be evaluated. Within errors the function is found to be independent of p_T , but it depends on p_L^* in the following way:

$$w(p_L^*) = \begin{cases} 0.868 + 0.270 \times p_L^* & \text{for } p_L^* < 0.5 \text{ GeV/c} \\ 1. & \text{for } p_L^* \geq 0.5 \text{ GeV/c} \end{cases} \qquad (4)$$

This dependence is assumed to be valid also in the region B. Thus we have now a means to reconstruct all inclusive spectra for positive pions.

Subtracting the obtained π^+ spectra from the total spectra of all positive particles, we get the corresponding proton spectra.

III. Inclusive Distributions

For π^+ mesons and protons the integrated single particle inclusive cross sections and average multiplicities are given in *table 1*.

Table 1
Intergated single particle cross section $\sigma_c = \langle n_c \rangle \sigma_{inel}$ and average multiplicity of particle c

Particle	σ_c (mb)	$\langle n_c \rangle$
π^+	72.87 ± 0.57	I.9I ± 0.02
p	I5.46 ± 0.57	0.4I ± 0.02

In *fig. 2* (and *fig. 3*) the invariant cross section for π^+'s is plotted as a function of x and p_T^2 (y^* and p_T^2) for different intervals of p_T. The double differential distributions exhibit an increasing backward shift of the maximum with increasing p_T. This effect contributes to the forward-backward asymmetry in the π^+ and π^- momentum distributions in the cms and has earlier been studied in terms of the average charge as a function of p_T in the central region. It has been found that the charge asymmetry increases with p_T [5].

The energy behaviour of $d\sigma/dy^*$ at fixed y^* for π^+'s can be studied from *fig. 4*, where the $\bar{p}p$ data at 5.7 *GeV/c* [6] and at 100 *GeV/c* [7] are also presented. In contrast to the pp data, where the invariant cross section for charged pion production at $y^* = 0$ rises

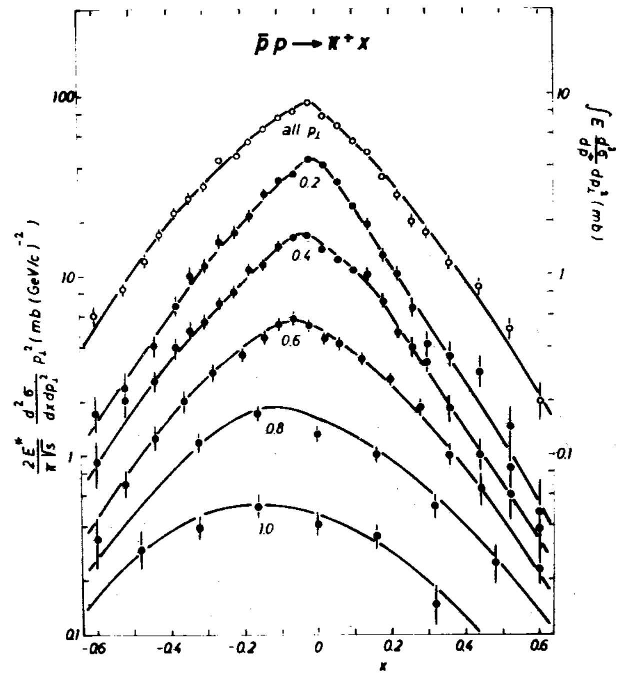

Fig. 2. Invariant cross section as a function of x *for different intervals of* p_T *for* π^+s*. The tompost data points have been obtained by integrating over* p_T*. The curves are drawn by hand.*

from 24 *GeV/c* to 200 *GeV/c* by about 40% [8], no energy variation is seen. The cross sections for the central ($y^* = 0$) and fragmentation ($y_{lab} = 0$) regions are given in *table 2*.

Because of a small number of inclusive protons (see *table 1*) we study the proton distributions only in single differential form. *Figure 5* shows the y^* distribution for protons.

e

The invariant inclusive cross sections $E \frac{d^3\sigma}{d\vec{p}}$ for π^+'s are given in *table 3* for different intervals of p_T and y^*.

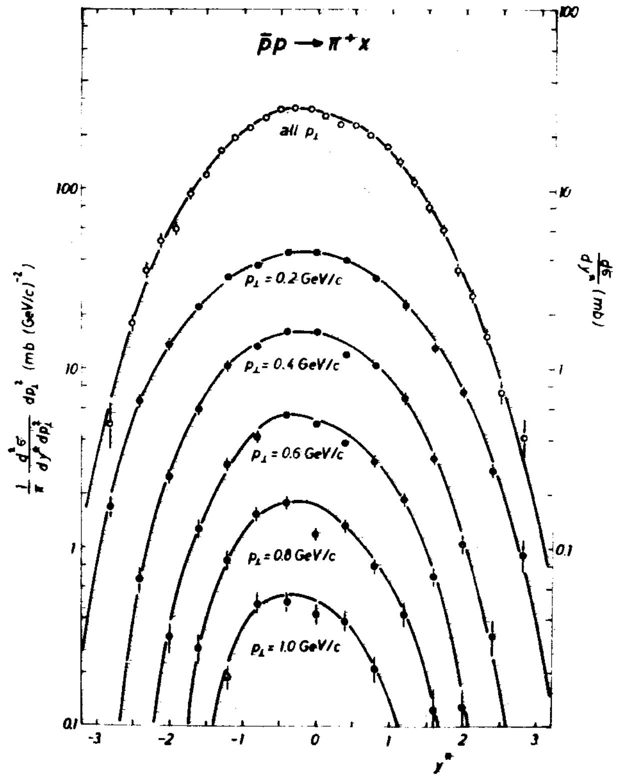

Fig. 3. Invariant cross section as a function of y^* *for different intervals of* p_T *for* π^+. *The topmost data points have been obtained by integrating over* p_T. *The curves are drawn by hand.*

The $d\sigma/dp_T^2$ distributions for π^+'s and p's are shown in *fig. 6*. When comparing the π^+ distribution with pions from the pp data at 24 *GeV/c* [9], we see that they are similar in shape. The ratio of

at 22.4 *GeV/c* to $pp \to \pi^- X$ at 24 *GeV/c* is shown in the lower part of *fig. 6*. This is close to the value 2.08 which is the ratio of the average π^- multiplicities. Statistical moments are given in *table 4*, where the $\bar{p}p$ data at 12 *GeV/c* [10] and 5.7 *GeV/c* [6] are also shown. For π^+'s the first two momentum increase with energy. In the

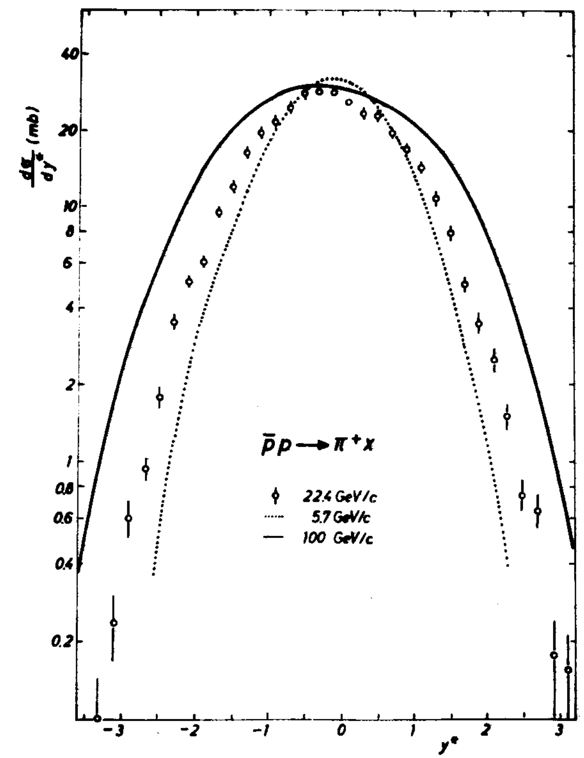

Fig. 4. Invariant cross section $d\sigma/dy^*$ *for* π^+'s. *The data at 100 GeV/c* [7] *and at 5.7 GeV/c* [6] *are also shown. The curves are drawn by hand.*

Table 2

Cross sections in *mb* in the central and fragmentation regions

Particle	$y^* = 0$	$y_{lab} = 0$
π^+	26.95 ± 0.78	6.97 ± 0.37
π^-	26.95 ± 0.78	3.70 ± 0.28
p	0.88 ± 0.62	9.03 ± 0.42

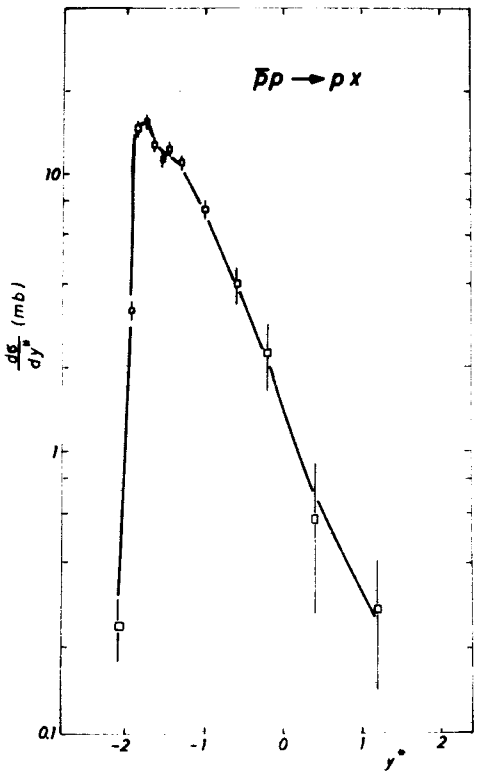

Fig. 5. Invariant cross section $d\sigma/dy^*$ *for* p's. *The curve is drawn by hand.*

proton case $\langle p_T^2\rangle$ increases, but $\langle p_T\rangle$ remains constant. The exponential slope for the proton distribution in an interval of 0.3 $(GeV/c)^2 \leq p_T^2 \leq$ 1.2 $(GeV/c)^2$ is smaller than that for π^+'s .

The x distribution for π^+ production as a function of the prong number (see *fig. 7*) indicates that the main contribution to the single differential spectra comes from 4- and 6-prong events. Topologies with $\geq$ 6 prongs have a maximum at $x \sim 0$ with an approximately exponential fall off along both sides of the distribution. Especially the maximum of two-prong events is shifted to the negative x values suggesting that π^+'s are fragmentation pro-

Table 3

Inclusive π^+ cross section $E\,\frac{d^3\sigma}{dp^3}$ $(mb(GeV/c)^{-2})$

y^* \ P_T	0 - 0.3	0.3 - 0.5	0.5 - 0.7	0.7 - 0.9	0.9 - 1.0
-2.8	1.71 ± 0.26				
-2.4	6.56 ± 0.52	0.674 ± 0.116			
-2.0	13.36 ± 0.76	2.49 ± 0.23	0.315 ± 0.066		
-1.6	21.95 ± 1.00	5.92 ± 0.36	1.28 ± 0.13	0.276 ± 0.053	
-1.2	31.81 ± 1.19	10.55 ± 0.48	2.93 ± 0.20	0.856 ± 0.093	0.193 ± 0.029
-0.8	36.90 ± 1.30	13.48 ± 0.55	4.20 ± 0.24	1.55 ± 0.11	0.493 ± 0.052
-0.4	44.49 ± 1.43	16.49 ± 0.62	5.64 ± 0.26	1.78 ± 0.13	0.503 ± 0.057
0.	43.78 ± 1.44	16.16 ± 0.60	4.93 ± 0.26	1.20 ± 0.11	0.428 ± 0.059
0.4	40.04 ± 1.36	12.22 ± 0.53	3.88 ± 0.24	1.35 ± 0.12	0.392 ± 0.059
0.8	32.00 ± 1.21	10.47 ± 0.50	3.13 ± 0.22	0.797 ± 0.093	0.212 ± 0.041
1.2	23.12 ± 1.03	6.90 ± 0.40	1.87 ± 0.17	0.431 ± 0.071	0.098 ± 0.030
1.6	13.24 ± 0.77	3.14 + 0.26	0.700 ± 0.101	0.125 ± 0.036	
2.0	7.47 ± 0.58	1.04 + 0.15	0.130 ± 0.044		
2.4	2.76 ± 0.34	0.327 ± 0.082			
2.8	0.939 ± 0.190				

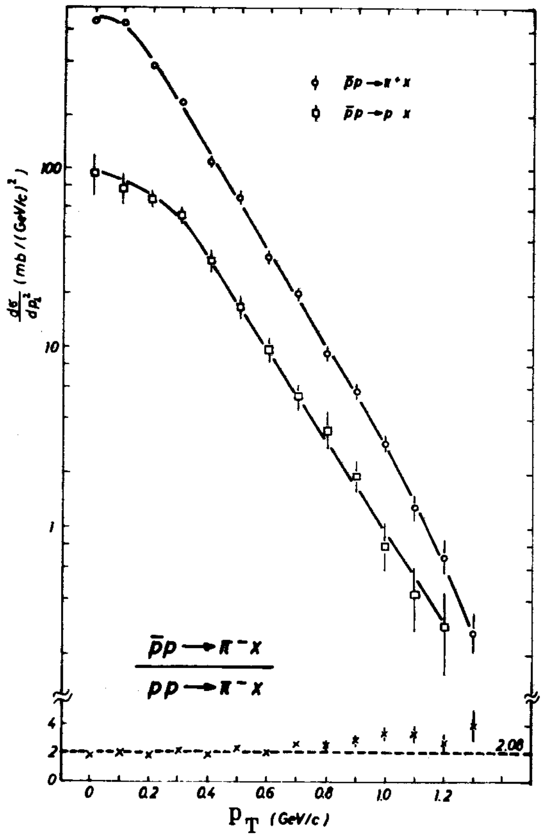

Fig. 6. Invariant cross section $d\sigma/dp_T^2$ *for* π^+*'s and* p *'s . The curves are drawn by hand. In the lower part of the figure, the ratio of* $d\sigma/dp_T^2$ *for* $\bar{p}p \to \pi^-$ *at 22.4 GeV/c and for* $\bar{p}p \to \pi^-$ *at 24 GeV/c is plotted. The value 2.08 is the ratio of the corresponding average multiplicities* .

ducts from the target particle. This effect is seen also in the distribution for four-prong events.

In *fig.8a* the x distribution for protons shows a clear diffraction peak around x = -0.9. From comparison with protons from the $\bar{p}p$ reactions at 12 *GeV/c* [10] and 5.7 *GeV/c* [6] we can see an increasing importance of

Table 4

Average characteristics of transverse momenta in $\bar{p}p$ interactions

Momentum (GeV/c)	Particle	$\langle p_T \rangle$ GeV/c	$\langle p_T^2 \rangle$ GeV/c^2	$D = (\langle p_T^2 \rangle - \langle p_T \rangle^2)^{1/2}$ GeV/c
22.4	π^+	0.334±0.002	0.162±0.002	0.225±0.002
	p	0.396±0.003	0.207±0.003	0.224±0.003
12.0	π^+	0.319±0.001		
	p	0.408±0.004		
5.7	π^+		0.144±0.004	
	p		0.175±0.003	

The errors are statistical.

the diffraction processes as the energy increases. The diffraction peak is shifted towards smaller x -values at higher energy. The diffraction peak is mostly due to two-prong events (see *fig. 8b*).

IV. Estimation of the Annihilation Component

In integrated quantities, such as total cross sections, mean multiplicities and higher multiplicity moments, annihilation reactions have been shown to be well approximated by the difference between $\bar{p}p$ and pp reactions [11]. This motivates a further assumption that differential quantities for annihilation reactions can be also estimated from the difference ($\bar{p}p - pp$). One can get only the total charged pion spectra in a straightforward way because $\bar{p}p$ reactions are charge asymmetric and pp reactions are charge symmetric in the cms. To get the π^+ and π^- distributions separately, one more assumption has been made [12], namely a relative excess of π^+ mesons over π^- mesons, or vice versa, in any part of phase space is independent of that whether the pions are produced in an annihilation or a non-annihilation

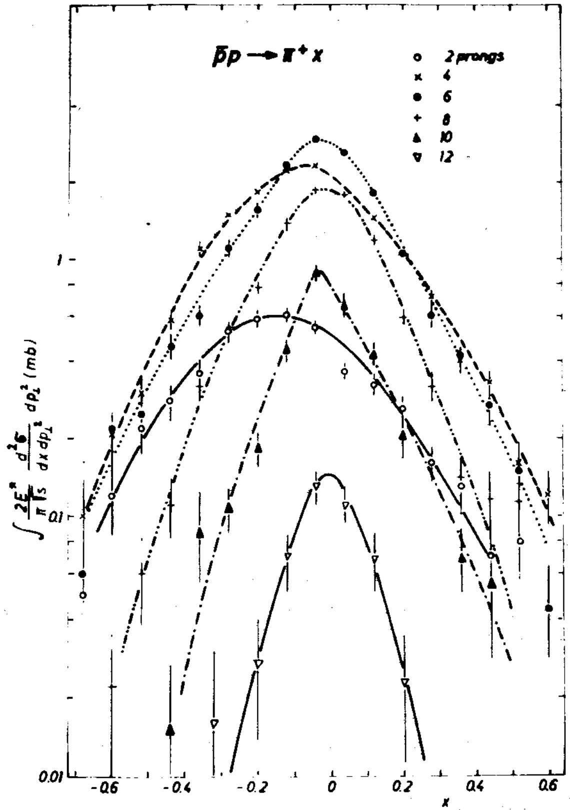

Fig. 7. Invariant cross section as a function of x *for different multiplicities for* π^+*'s. The curves are drawn by hand.*

reaction. The formula for the annihilation invariant inclusive cross section can be written as

$$f_{ann}(\bar{p}p \to \pi^{\pm}) = \frac{f(\bar{p}p \to \pi) - f(pp \to \pi)}{f(\bar{p}p \to \pi)} \times f(\bar{p}p \to \pi^{\pm}). \quad (5)$$

This relation has been compared with the true annihilation data at 12 *GeV/c*, and a very good agreement with them justifies it at least at this energy [12].

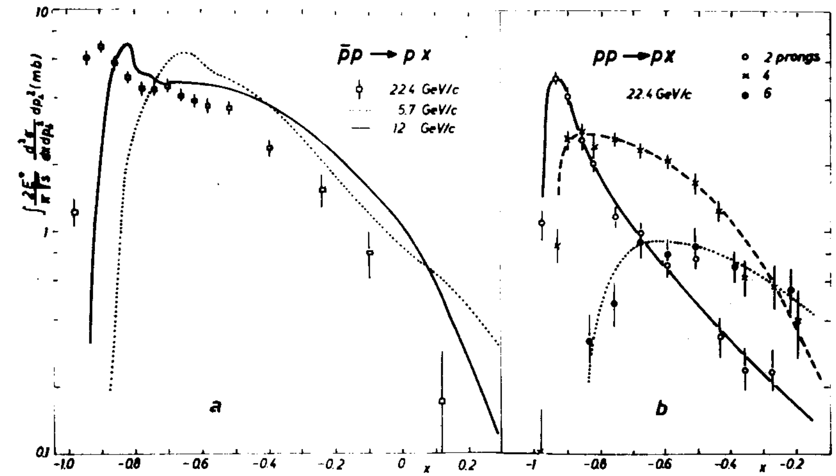

Fig. 8. Invariant cross section as a function of x *for* p's *: (a) for all events, the 12 GeV/c* [10] *and 5.7 GeV/c* [6] *data have been added; (b) for the topologies 2, 4 and 6. The curves are drawn by hand.*

In *fig. 9a* the invariant cross section for the difference between the charged pion spectra in our data and the pp data at 24 *GeV/c* [9] is shown as a function of y^* and p_T. We can see universality in the shape of the invariant inclusive pion spectra for the pp and ($\bar{p}p - pp$) data. With increasing p_T the ($\bar{p}p - pp$) cross section becomes more important and at $p_T \sim 1$ *GeV/c* it starts to dominate over the pp cross section. In *fig. 9b* we show the corresponding π^+ spectrum as obtained from eq. (5). The increasing charge asymmetry as a function of p_T is also seen here as expected because of a stronger effect in $\bar{p}p$ than in pp data [5].

V. Conclusions

Investigating the inclusive spectra of π^+ mesons and protons in $\bar{p}p$ interactions at 22.4 *GeV/c* we reached the following results:

1. The average multiplicity for π^+ meson (proton) production is 1.92±0.02 (0.41±0.02).

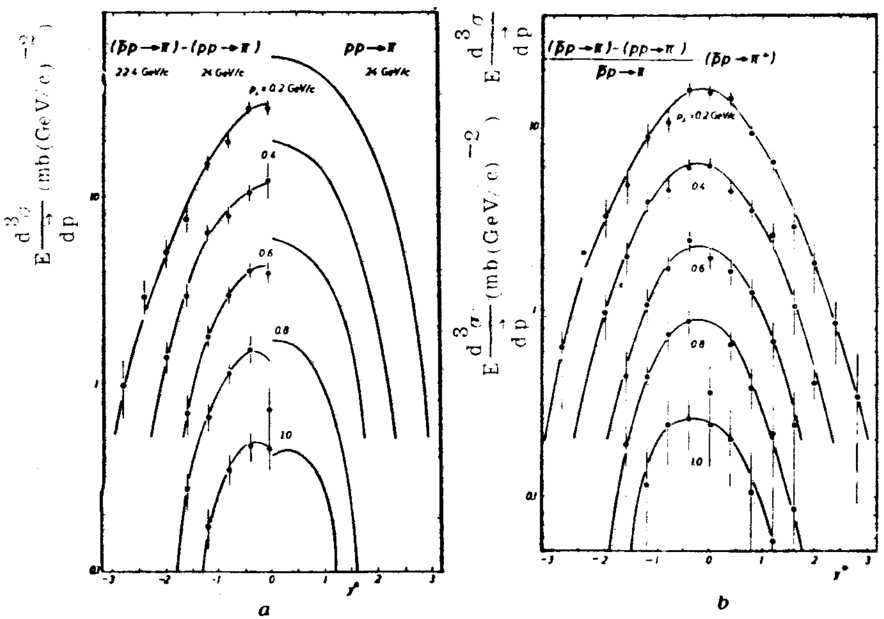

Fig. 9. Invariant cross section $E\frac{d^3\sigma}{d\vec{p}}$ *(a) for the difference of the total pion production of* $\bar{p}p\to\pi$ *at 22.4 GeV/c and* $pp\to\pi$ *at 24 GeV/c* [9] *(backward hemisphere) and the source data for* $pp\to\pi$ *(forward hemisphere); (b) for the annihilation pions* $(\bar{p}p\to\pi^+)$ *estimated according to eq. (5) (see text) for different* p_T *intervals.*

2. In contrast to the pp reaction, the energy variation of the $d\sigma/dy^*$ distribution at $y^*=0$ for π^+ production in $\bar{p}p$ interactions is very small between 5.7 and 100 *GeV/c*.

3. We observe universality in the shape of the invariant inclusive spectra for π^+ mesons in the $\bar{p}p$ and pp re-inclusive spectra for π^+ mesons in the $\bar{p}p$ and pp reactions as well as in the spectra obtained from eq. (5) which can be a good approximation for the annihilation distributions.

The authors want to express their gratitude to the staff responsible for the operation of the Serpukhov accelerator and of the beam channel no. 9 and to the technical staff of the "Ludmila" bubble chamber. We also thank the technicians and assistants at all laboratories for their excellent work.

References

1. *Abesalashvili L.N. et al. Phys.Lett., 1974, 52B, p.236.*
2. *Boos E.G. et al. Nucl.Phys., 1977, B121, p. 381.*
3. *Antipov Yu.M. et al. Nucl.Phys., 1973, B57, p. 333.*
4. *Bracci E. et al. CERN/HERA 73-1 (1973).*
5. *Boos E.G. et al. JINR, E1-10453, Dubna, 1977; Nucl.Phys., 1977, B123, p. 269.*
6. *Chýla J. et al. Thesis, Institute of Physics, CSAV, Prague, 1976.*
7. *Neale W.W. Analysis of Antiproton Reactions at 100 GeV/c, Proceedings of the EPS International Conference, Palermo, June, 1975, p. 1007. Whitemore J. et al. Phys.Rev.Lett., 1977, 38, p. 996.*
8. *Böckmann K. Single Particle and Multiplicity Distributions, Proceedings of the EPS International Conference, Palermo, June 1975, p. 794.*
9. *Blobel V. et al. Nucl.Phys., 1974, B69, p. 454.*
10. *Gall D. et al. Particle and Resonance Production in* p̄p *Interactions at 12 GeV/c, Proceedings of the International Symposium on* p̄p *-Interactions, Loma-Koli, Finland, June 1975, p. 414.*
11. *Whitemore J. Phys.Report, 1976, 27C, p. 187.*
12. *Raja R. Preprint FERMILAB-Pub-76/99-EXP, Batavia, Dec. 1976.*

Received by Publishing Department
on February 16, 1978.